

Solar kerosene from H₂O and CO₂

P. Furler, D. Marxer, J. Scheffe, D. Reinalda, H. Geerlings, C. Falter, V. Batteiger, A. Sizmann, and A. Steinfeld

Citation: [AIP Conference Proceedings](#) **1850**, 100006 (2017); doi: 10.1063/1.4984463

View online: <http://dx.doi.org/10.1063/1.4984463>

View Table of Contents: <http://aip.scitation.org/toc/apc/1850/1>

Published by the [American Institute of Physics](#)

Articles you may be interested in

[Perspectives of advanced thermal management in solar thermochemical syngas production using a counter-flow solid-solid heat exchanger](#)

AIP Conference Proceedings **1850**, 100005 (2017); 10.1063/1.4984462

[Solar hydrogen production with cerium oxides thermochemical cycle](#)

AIP Conference Proceedings **1850**, 100002 (2017); 10.1063/1.4984459

[Solar fuels production as a sustainable alternative for substituting fossil fuels: COSOL \$\pi\$ project](#)

AIP Conference Proceedings **1850**, 100015 (2017); 10.1063/1.4984472

[A-site substitution effect of perovskite-type cobalt and manganese oxides on two-step water splitting reaction for solar hydrogen production](#)

AIP Conference Proceedings **1850**, 100011 (2017); 10.1063/1.4984468

[A solar fuels roadmap for Australia – study outcomes](#)

AIP Conference Proceedings **1850**, 100010 (2017); 10.1063/1.4984467

[Development and experimental study for hydrogen production from the thermochemical two-step water splitting cycles with a CeO₂ coated new foam device design using solar furnace system](#)

AIP Conference Proceedings **1850**, 100003 (2017); 10.1063/1.4984460



SUMMER SALE!

30% OFF
ALL PRINT
PROCEEDINGS!

AIP | Conference Proceedings

ENTER COUPON CODE
SUMMER2017

Solar Kerosene from H₂O and CO₂

P. Furler¹, D. Marxer¹, J. Scheffe¹, D. Reinalda², H. Geerlings², C. Falter³,
V. Batteiger³, A. Sizmann³ and A. Steinfeld^{1, a)}

¹Department of Mechanical and Process Engineering, ETH Zurich, 8092 Zurich, Switzerland

²Shell Global Solutions International B.V., 1031 HW Amsterdam, The Netherlands

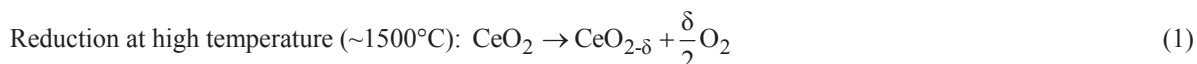
³Bauhaus Luftfahrt e.V., 80807 München, Germany

^{a)}Corresponding author: aldo.steinfeld@ethz.ch

Abstract. The entire production chain for renewable kerosene obtained directly from sunlight, H₂O, and CO₂ is experimentally demonstrated. The key component of the production process is a high-temperature solar reactor containing a reticulated porous ceramic (RPC) structure made of ceria, which enables the splitting of H₂O and CO₂ via a 2-step thermochemical redox cycle. In the 1st reduction step, ceria is endo-thermally reduced using concentrated solar radiation as the energy source of process heat. In the 2nd oxidation step, nonstoichiometric ceria reacts with H₂O and CO₂ to form H₂ and CO – syngas – which is finally converted into kerosene by the Fischer-Tropsch process. The RPC featured dual-scale porosity for enhanced heat and mass transfer: mm-size pores for volumetric radiation absorption during the reduction step and μm-size pores within its struts for fast kinetics during the oxidation step. We report on the engineering design of the solar reactor and the experimental demonstration of over 290 consecutive redox cycles for producing high-quality syngas suitable for the processing of liquid hydrocarbon fuels.

INTRODUCTION

Solar-driven thermochemical cycles based on metal oxide redox reactions can split H₂O and CO₂ to produce H₂ and CO (syngas), the precursors to the catalytic synthesis of conventional liquid fuels for the transportation sector.^{1,2,3,4} In contrast to the thermolysis, these cycles bypass the CO/O₂ and H₂/O₂ separation problem. When coupled to the capture of CO₂ directly from atmospheric air, the solar-made hydrocarbon fuels can be considered carbon neutral.^{5,6,7,8} Today, the state-of-the-art material for thermochemical cycling is nonstoichiometric ceria (CeO_{2-δ}) due to its fast reaction kinetics and crystallographic stability over a wide range of oxidation states.^{9,10,11} The two-step H₂O/CO₂ splitting cycle based on nonstoichiometric ceria is represented by:



The first step proceeds via the thermal reduction of CeO₂ to a non-stoichiometric state, and O₂ is evolved.^{12,13} The reduced ceria is then re-oxidized in the second lower-temperature step using steam or CO₂ to produce H₂, CO, or a synthesis gas mixture (CO and H₂).^{14,15} The net inputs are solar energy, water, and CO₂. The net reactions are H₂O = H₂ + ½ O₂ and/or CO₂ = CO + ½ O₂. The morphology of the ceria structure for the 2-step cycle has a significant impact on the energy efficiency of the process.^{16,17} We showed in previous experimental campaigns that the high-temperature reduction step according to Eq. 1 is limited by heat transfer,¹⁶ while the oxidation step according to Eq. 2 is limited by the available surface area of the structure.¹⁸ Therefore, the desired ceria structure should combine low optical thickness to enable fast and homogeneous heating by concentrated radiation, sufficiently high specific surface area to guarantee fast reaction kinetics for the oxidation with H₂O and/or CO₂, and high mass

loading. Hence, we have engineered a reticulated porous ceramic (foam-type) structure made of ceria with dual-scale porosity in the millimeter and micrometer ranges. The larger void size range, with $d_{\text{mean}} = 2.5$ mm and porosity = 0.76 – 0.82, enables volumetric absorption of concentrated solar radiation for efficient heat transfer to the reaction site during endothermic reduction, while the smaller void size range within the struts, with $d_{\text{mean}} = 10$ μm and strut porosity up to 0.44, increases the specific surface area for enhanced reaction kinetics during exothermic oxidation with H_2O and/or CO_2 .¹⁸

In this work, we used the dual-scale ceria RPC in a solar reactor and performed 291 consecutive redox cycle. The produced synthesis gas was subsequently further processed via Fischer-Tropsch synthesis in order to demonstrate experimentally the entire production chain to renewable kerosene.

EXPERIMENTAL SECTION

Experimental Setup and Methods

The experimental setup consisting of (a) the high-flux solar simulator, (b) the solar reactor, (c) the gas compression unit, (d) the Fischer-Tropsch system, and peripheries are schematically shown in Fig. 1. The solar reactor, which is the core component of the setup, was previously described in detail;^{14,15,16,17} the main features are summarized here. It consisted of a cavity-receiver with a 4 cm-diameter aperture for the access of concentrated solar radiation. The reactor front was sealed by a 24 cm-diameter, 3 mm-thick clear fused quartz disk window. A compound parabolic concentrator (CPC¹⁹) was incorporated onto the aperture to further boost the solar concentration ratio to mean values of up to 3000 suns. The ceria RPC was contained within the cavity as a cylinder composed of four 20 mm-thick, 60 mm-i.d., 100 mm-o.d. rings and a single 20 mm-thick, 100 mm-o.d. disk. The total mass of the CeO_2 cylinder was 948 g. The cavity was insulated by Al_2O_3 and sheathed by an outer shell made of Inconel 600. An annular gap between the RPC and insulation enabled uniform radial flow across the porous RPC cylinder. Temperatures were measured at the outer surface of the RPC (B-type thermocouples), insulation, and Inconel wall (K-type thermocouples). Argon (99.999% purity) and CO_2 (99.998% purity) flow rates were regulated by electronic mass flow controllers (Bronkhorst F-201C). Reacting gases were injected through four radial inlet ports and product gases exited the reactor axially through an outlet port at the rear plate. Product gas composition was monitored by gas chromatography (Varian 490), supplemented by a paramagnetic alternating pressure based O_2 detector (Siemens Oxyamat 6) and infrared-based detectors for CO and CO_2 (Siemens Ultramat).

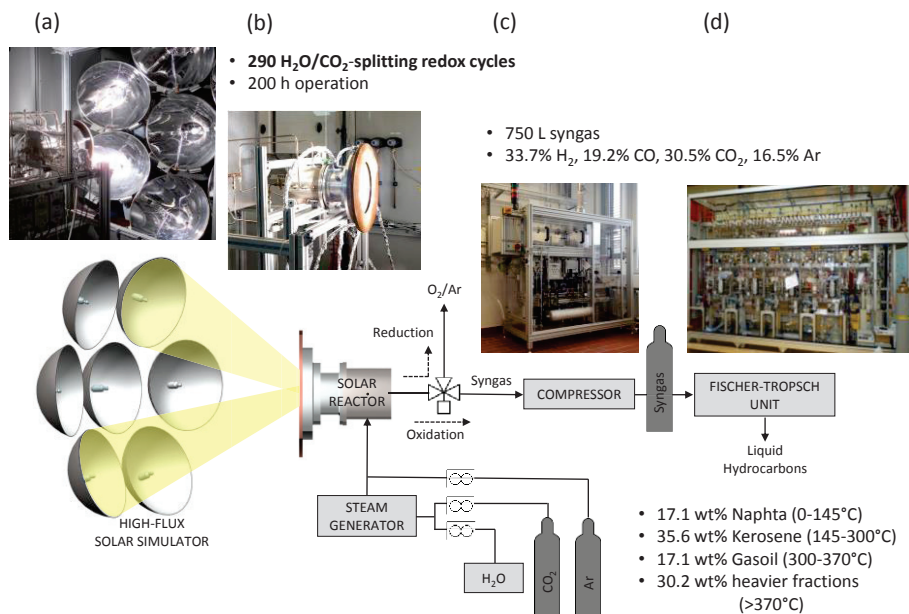


FIGURE 1. Schematic and pictures of the main system components of the production chain to solar kerosene from H_2O and CO_2 via the ceria-based thermochemical cycle. (a) High-Flux Solar Simulator, (b) solar reactor, (c) gas compressing unit, and (d) Fischer-Tropsch system.¹⁷

Experimentation was performed at the High-Flux Solar Simulator (HFSS) of ETH Zurich. An array of seven Xe-arcs, close-coupled to truncated ellipsoidal reflectors, provided an external source of intense thermal radiation, mostly in the visible and IR spectra, that closely approximated the heat transfer characteristics of highly concentrating solar systems such as solar towers and dishes.²⁰ The radiative flux distribution at the focal plane was measured optically using a calibrated CCD camera focused on a water-cooled, Al₂O₃-plasma coated Lambertian (diffusely reflecting) target. The solar radiative power input through the aperture P_{solar} was calculated by integration of the radiative flux over the aperture area and verified with a water-calorimeter.

During a typical redox cycle, the reactor was heated by $P_{\text{solar}} = 2.8\text{-}3.8$ kW to the desired reduction temperature in the range 1450-1600 °C while purging with Ar flow rates \dot{V}_{Ar} ranging from 2 to 10 L min⁻¹. Following reduction, the HFSS was turned off ($P_{\text{solar}} = 0$) and the reactor was cooled to the desired oxidation temperature in the range 700-1200 °C. Subsequently, oxidation was performed at $P_{\text{solar}} = 0\text{-}0.8$ kW by injecting the reactant gases, either CO₂ or a mixture of CO₂ and H₂O. The product gas was collected in a gas sample bag (SKC series 263-50) and compressed to 150 bar.

The solar syngas collected was analyzed for catalyst poisons by proton-transfer-reaction mass spectrometry (PTR-MS) in the H₃O⁺ mode at 600 V drift chamber voltage (Ionicon Analytik GmbH, Innsbruck, Austria). Electron micrographs were recorded on a Hitachi TM-1000 at an acceleration voltage of 15 kV. Mercury porosimetry was performed on a Quantachrome Poremaster 60-GT (Quantachrome GmbH + Co KG, Odelzhausen, Germany). Liquid fuel synthesis of the solar-made syngas was performed via the Fischer-Tropsch process at Shell Global Solutions, Amsterdam.

Materials

Ceria RPC parts with dual-scale porosity were fabricated by the replication method.²¹ Cerium (IV)-oxide powder (particle size < 5 μm, 99.9% purity, Sigma Aldrich) was mixed with water in a 5:1 mass ratio, 30 Vol-% of spherical carbon pore-forming agent particles (particle size 0.4-12 μm, HTW Hochttemperatur-Werkstoffe GmbH), 0.83 wt-% organic deflocculating agent (Dolapix CE 64), polyvinyl alcohol binder (Optapix RA 4G), and antifoaming agent (Contraspum KWE), and processed according to a previously published recipe.^{18,22} Organic polyurethane sponges of 10 ppi (Foam-Partner, Fritz Nauer AG) were then immersed into the slurry, which was dried in air and finally sintered in an electrically heated furnace at 1600 °C.²²

RESULTS AND DISCUSSION

Figure 2 shows the nominal solar reactor temperature at the end of the reduction step and the peak CO and H₂ evolution rates for 291 redox cycles performed with the solar reactor.¹⁷ The first 60 cycles (shown in Fig. 2 region I and II) were performed under varying experimental conditions ($P_{\text{solar}} = 2.8\text{-}3.8$ kW during reduction, $P_{\text{solar}} = 0\text{-}0.8$ kW during oxidation, and $\dot{V}_{\text{Ar}} / \dot{V}_{\text{CO}_2} = 0.5\text{-}10$ L min⁻¹, $\dot{V}_{\text{H}_2\text{O}} = 2\text{-}4$ L min⁻¹), to examine the performance of the solar reactor and to find appropriate baseline conditions for cyclic operation. The scattered results during cycles 1-60 were due to the effect of varying such conditions in an effort to increase throughput and total syngas concentration. Co-feeding a mixture of H₂O and CO₂ at a molar ratio of 4.8 and a total flow rate of 2.9 L min⁻¹ for 7-10 min resulted in syngas with a H₂:CO molar ratio of roughly 1.7 and a total syngas concentration above 50% in the product gas stream. This is in agreement with previous experimental results obtained with the solar reactor.¹⁵ Region III (cycles # 61-227) in Fig. 2 shows 167 consecutive H₂O/CO₂-splitting cycles where the reactor temperature was stabilized during oxidation at around 750 °C with $P_{\text{solar}} = 0.8$ kW and the oxidation was terminated when the syngas concentration dropped below 40%. Also indicated are linear fits of the nominal reactor temperature and H₂/CO production rates, which slightly decreased with cycle number. We attributed the decreasing temperature and rates to sintering of the insulation which shifted the RPC rings out of center, causing blocking and non-uniform absorption of incoming concentrated radiation. In addition, a slight decrease in specific surface area due to grain growth may have affected the peak rates, but this effect is marginal. Thus, the minor decrease in peak reaction rate is mainly attributed to the solar reactor itself rather than the chemical or morphological stability of the CeO₂. The chemical and morphological stability of porous CeO₂ samples has been experimentally studied by Chueh et al. in a well-controlled infrared furnace.^{10,14} 500 H₂O splitting cycles with CeO₂ were performed, yielding a remarkable stability of H₂/O₂ yields and rates. Only during the first 100 cycles a drop in yields and rates was observed and attributed to sintering and grain growth (morphological change).

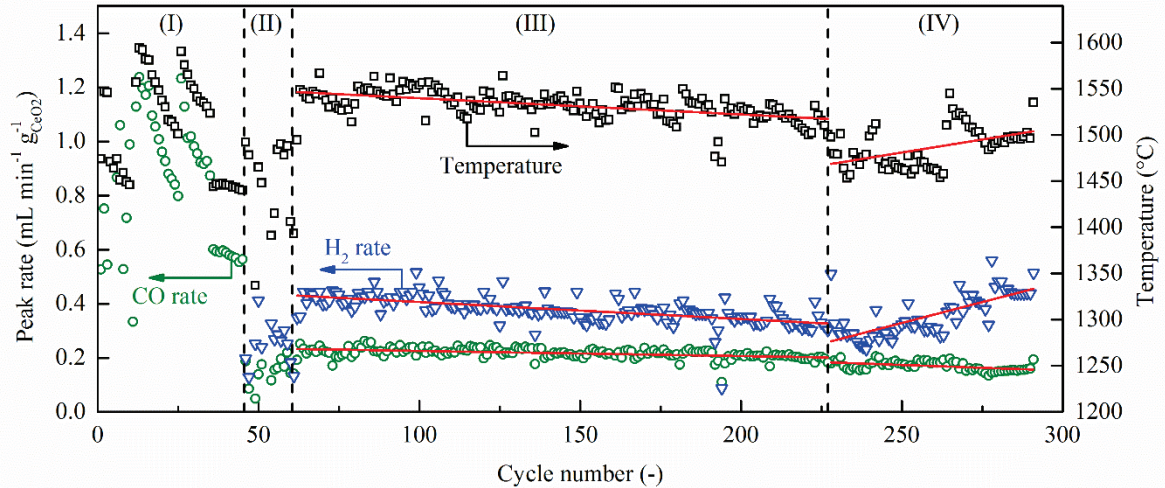


FIGURE 2. Nominal solar reactor temperature at the end of the reduction step and peak CO and H₂ production rates for 291 redox cycles performed with the solar reactor. Region I and II represent redox cycles performed under varying experimental conditions to find appropriate baseline conditions for cyclic operation. Region II (cycles #46-60): H₂O/CO₂-splitting cycles at $P_{\text{solar}} = 3.8$ kW during reduction, $P_{\text{solar}} = 0$ kW during oxidation, and various flow configurations. Region III (cycles # 61-227): 167 consecutive H₂O/CO₂-splitting cycles at $P_{\text{solar}} = 3.8$ kW and $\dot{V}_{\text{Ar}} = 8$ L min⁻¹ for 20 min during reduction, 8 min cooling, and $P_{\text{solar}} = 0-0.8$ kW at 750 °C with $\dot{V}_{\text{CO}_2} = 0.5$ L min⁻¹ and $\dot{V}_{\text{H}_2\text{O}} = 2.4$ L min⁻¹ for 8 min during oxidation. Region IV (cycles #228-291): 64 consecutive H₂O/CO₂-splitting cycles at similar operating conditions as in Region III but with fresh RPCs. Figure extracted from Ref. 17.

Region IV (cycles # 228-291) in Fig. 2 shows 64 consecutive cycles performed under similar operating conditions as in Region III but with fresh RPCs. Here we observed increasing reactor temperatures and H₂ rates with cycle number. The former is attributed to an increase of the time duration of the reduction step in an effort to maximize δ and total syngas throughput (rather than efficiency $\eta_{\text{solar-to-fuel}}$). The latter is attributed to an increasing H₂O:CO₂ co-feeding ratio to obtain higher H₂:CO ratio in the collected syngas. The total syngas production rate increased from cycle to cycle which indicated the strong effect of the solar reactor temperature during thermal reduction on the fuel output per cycle.

SEM images revealed grain growth and moderate sintering, but no loss in open porosity was detected as depicted in Fig. 3. Preservation of the open porosity was confirmed by mercury intrusion porosimetry measurements, which indicated open strut porosity before and after 227 cycles of 24% and 23%, respectively. Overall, the RPC exhibited superior stability over multiple cycling under solar concentrating conditions.

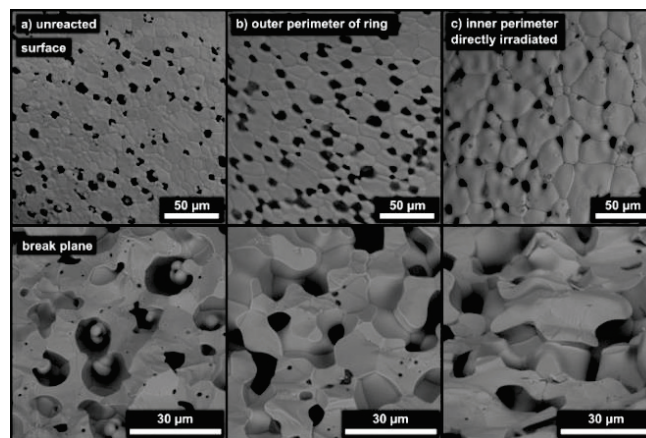


FIGURE 3. SEM micrographs of strut surfaces (top) and break planes (bottom) of samples: a) freshly produced RPC; b) outer perimeter of an RPC ring after 227 cycles; and c) directly irradiated inner perimeter of an RPC ring after 227 cycles. Figure taken from Ref 17.

The syngas produced during 231 cycles (regions III and IV of Fig. 2) was collected and compressed into a 5 L standard aluminum gas bottle by the compression unit depicted in Fig. 1 (c) to a final pressure of 150 bar at room temperature. This corresponded to 700 standard liters of syngas with a final composition of 33.7% H₂, 19.2% CO, 30.5% CO₂, 0.06% O₂, 0.09% CH₄, and 16.5% Ar. Unreacted H₂O was condensed and separated. Adverse poisons for FT-catalysts were not detected at a lower detection limit (LOD) of 1 ppb by PTR-MS. The trace amount of O₂ was presumably due to O₂ still trapped in the pipes when switching from reduction to oxidation mode, while CH₄ was likely formed by methanation on catalytic metallic surfaces. The H₂:CO molar ratio was 1.76, which fits the targeted syngas quality for FT-synthesis, proving the good controllability of the process.

The collected syngas was subsequently processed via FT and hydrocracking at Shell Global Solutions, Amsterdam, yielding liquid hydrocarbons with the following composition: 17.1 wt% naphtha (boiling range 0-145 °C), 35.6 wt% kerosene (145-300 °C), 17.1 wt% gasoil (300-370 °C), and 30.2 wt% of heavier fractions (>370 °C). This is the first ever production of jet fuel by solar thermochemical splitting of CO₂ and H₂O. No attempt was undertaken to optimize the gas-to-liquid process. The selectivity to kerosene can be made to exceed 50%.

The results of this experimental campaign demonstrated the technical feasibility of the solar redox process at operating conditions relevant to industrial scale implementation.

SUMMARY AND CONCLUSIONS

291 consecutive CO₂ and CO₂/H₂O splitting cycles based on non-stoichiometric ceria have been performed in a solar reactor, yielding 700 standard liters of syngas of composition suitable for direct gas-to-liquid processing via FT. Chemical yields and rates were largely stable over the course of the consecutive cycles. SEM images revealed grain growth and moderate sintering, but no loss in open porosity was detected. To the best of our knowledge, this was the first experimental coupling of solar syngas production from H₂O and CO₂ with the storage, compression, and FT-processing to liquid hydrocarbons. FT-processed kerosene, derived from H₂O and CO₂, can be certified for commercial aviation by minor addendum to the existing D7566 specification for synthesized hydrocarbons.

ACKNOWLEDGEMENTS

This work has been financially supported by the European Commission under contract No. 285098 – Project SOLAR-JET, and by the Swiss Competence Center Energy & Mobility. We thank Dr. Ulrich Vogt, Michal Gorbar, and Alexander Bonk at EMPA for their support with the RPC fabrication.

NOMENCLATURE AND ABBREVIATIONS

d_{mean} = mean pore size (m)
 C = solar flux concentration ratio
 I = direct normal solar irradiation (W m⁻²)
 P_{solar} = solar radiative power (W)
 T = temperature (°C)
 δ = non-stoichiometry
 $\eta_{\text{solar-to-fuel}}$ = solar-to-fuel energy conversion efficiency
 V_{v} = volumetric flow rate (L min⁻¹)

CCD = charge-coupled device
CPC = compound parabolic concentrator
FT = Fischer-Tropsch
HFSS = high flux solar simulator
L = standard liters (at 273.15 K and 1 atm)
LOD = lower limit of detection
ppb = parts per billion
PTR-MS = proton transfer reaction-mass spectrometry
RPC = reticulated porous ceramic
SEM = scanning electron microscopy

REFERENCES

1. A. Steinfeld, "Solar thermochemical production of hydrogen—a review," *Sol. Energy* **78**, 603–615 (2005).
2. G. P. Smestad and A. Steinfeld, "A. Review: Photochemical and Thermochemical Production of Solar Fuels from H₂O and CO₂ Using Metal Oxide Catalysts," *Ind. Eng. Chem. Res.* **51**, 11828–11840 (2012).
3. C. Perkins and A. W. Weimer, "Likely near-term solar-thermal water splitting technologies," *Int. J. Hydrogen Energy* **29**, 1587–1599 (2004).
4. C. Graves, S.D. Ebbesen, M. Mogensen, and K. S. Lackner, "Sustainable hydrocarbon fuels by recycling CO₂ and H₂O with renewable or nuclear energy," *Renew. Sustain. Energy Rev.* **15**, 1–23 (2011).
5. J. A. Wurzbacher, C. Gebald, and A. Steinfeld, "Separation of CO₂ from air by temperature-vacuum swing adsorption using diamine-functionalized silica gel," *Energy Environ. Sci.* **4**, 3584 (2011).
6. V. Nikulshina, C. Gebald, and A. Steinfeld, "CO₂ capture from atmospheric air via consecutive CaO-carbonation and CaCO₃-calcination cycles in a fluidized-bed solar reactor," *Chem. Eng. J.* **146**, 244–248 (2009).
7. K. S. Lackner, "Capture of carbon dioxide from ambient air," *Eur. Phys. J. Spec. Top.* **176**, 93–106 (2009).
8. C. Gebald, J. A. Wurzbacher, P. Tingaut, T. Zimmermann, and A. Steinfeld, "Amine-based nanofibrillated cellulose as adsorbent for CO₂ capture from air," *Env. Sci Technol* **45**, 9101–9108 (2011).
9. A. H. McDaniel, A. Ambrosini, E. N. Coker, J.E. Miller, W.C. Chueh, R. O'Hayre, and J. Tong, "Nonstoichiometric perovskite oxides for solar thermochemical H₂ and CO production," *Energy Procedia* **49**, 2009–2018 (2013).
10. W. C. Chueh and S. M. Haile, "A thermochemical study of ceria: exploiting an old material for new modes of energy conversion and CO₂ mitigation," *Philos Trans. A Math Phys Eng Sci* **368**, 3269–3294 (2010).
11. M. Zinkevich, D. Djurovic, and F. Aldinger, "Thermodynamic modelling of the cerium-oxygen system," *Solid State Ionics* **177**, 989–1001 (2006).
12. J. R. Scheffe and A. Steinfeld, "Thermodynamic Analysis of Cerium-Based Oxides for Solar Thermochemical Fuel Production," *Energy & Fuels* **26**, 1928–1936 (2012).
13. R. J. Panlener, R. N. Blumenthal, and J. E. Garnier, "A thermodynamic study of nonstoichiometric cerium dioxide," *J. Phys. Chem. Solids* **36**, 1213–1222 (1975).
14. W. C. Chueh, C. Falter, M. Abbott, D. Scipio, P. Furler, S. M. Haile, and A. Steinfeld, "High-flux solar-driven thermochemical dissociation of CO₂ and H₂O using nonstoichiometric ceria," *Science* **330**, 1797–1801 (2010).
15. P. Furler, J.R. Scheffe, and A. Steinfeld, "Syngas production by simultaneous splitting of H₂O and CO₂ via ceria redox reactions in a high-temperature solar reactor," *Energy Environ. Sci.* **5**, 6098 (2012).
16. P. Furler, J. R. Scheffe, M. Gorbar, L. Moes, U. Vogt, and A. Steinfeld, "Solar thermochemical CO₂ splitting utilizing a reticulated porous ceria redox system," *Energy & Fuels* **26**, 7051–7059 (2012).
17. D. Marxer, P. Furler, J. R. Scheffe, H. Geerlings, C. Falter, V. Batteiger, A. Sizmann, and A. Steinfeld, "Demonstration of the Entire Production Chain to Renewable Kerosene via Solar Thermochemical Splitting of H₂O and CO₂," *Energy & Fuels* **29**, 3241–3250 (2015).
18. P. Furler, J. R. Scheffe, D. Marxer, M. Gorbar, A. Bonk, U. Vogt, and A. Steinfeld, "Thermochemical CO₂ splitting via redox cycling of ceria reticulated foam structures with dual-scale porosities," *Phys. Chem. Chem. Phys.* **16**, 10503–11 (2014).
19. W. T. Welford and R. Winston, "High Collection Nonimaging Optics," Academic Press, San Diego, 1989.
20. J. Petrasch, P. Coray, A. Meier, M. Brack, P. Häberling, D. Wüillemin, and A. Steinfeld, "A Novel 50kW 11,000 suns High-Flux Solar Simulator Based on an Array of Xenon Arc Lamps," *J. Sol. Energy Eng.* **129**, 405 (2007).
21. K. Schwartzwalder and A. Somers, US Patent No. 3090094 A (1961).
22. U. Vogt, M. Gorbar, P. Dimopoulos-Eggenschwiler, A. Broenstrup, G. Wagner, and P. Colombo, "Improving the properties of ceramic foams by a vacuum infiltration process," *J. Eur. Ceram. Soc.* **30**, 3005–3011 (2010).